

## **MODEL UPDATING OF A MASONRY HISTORICAL CHURCH BASED ON OPERATIONAL MODAL ANALYSIS: THE CASE STUDY OF SAN FILIPPO NERI IN MACERATA**

**Carlo Baggio<sup>1</sup>, Valerio Sabbatini<sup>2</sup> and Silvia Santini<sup>3</sup>**

Roma Tre University

Department of Architecture, Largo Giovanni Battista Marzi 10, 00153, Rome, Italy

e-mail: <sup>1</sup>[carlo.baggio@uniroma3](mailto:carlo.baggio@uniroma3)

<sup>2</sup>[valerio.sabbatini@uniroma3.it](mailto:valerio.sabbatini@uniroma3.it)

<sup>3</sup> [silvia.santini@uniroma3.it](mailto:silvia.santini@uniroma3.it)

---

### **Abstract**

*The paper describes the approach followed in the characterization of the structural behavior of the historical masonry church of San Filippo Neri in Macerata, severely damaged and condemned after the Central Italy Earthquake occurred in October 2016. The case study of San Filippo Neri is particularly interesting: first for the historical and artistic importance of the church furthermore for the evidences of recurrent structural damage.*

*The laboratory of Proof and Research on Structures and Materials of Roma Tre University carried out an extensive onsite testing campaign – including geometric survey, flat-jack test and ambient vibration test – in order to investigate the state of the building. Operational modal analysis was used to assess the dynamic behavior of the church; the results of the testing campaign were interpreted and correlated with an accurate finite element model of the construction. The numerical model was finally tuned up based on the experimental results in order to match the dynamic behavior.*

*The aim of the research is to set the first steps for an integrated approach able to fit and combine the results from experimental onsite testing and numerical modelling.*

**Keywords:** Historical Masonry, Operational Modal Analysis, Ambient Vibration Test, Structural identification

---

## 1 INTRODUCTION

During the last decades, conservation and structural safety assessment of historical buildings gained great importance especially in seismic countries with significant architectural heritage. Italy comprise a heterogeneous and extended cultural heritage, its proper conservation has become a relevant concern particularly after the latest seismic events [1].

The prediction of the mechanical response of historical masonry constructions is a complex task to accomplish where the expected behavior of the building is often misleading from the real one [2]; different strategies have been developed to approach masonry structural analysis: simplified kinematic methods, FEM, limit analysis and discrete element methods are the most common and available, however the application of these methods requires accurate geometry and material characterizations which strongly influence the results [3].

After the occurrence of severe seismic events [4], it has been developed in the Italian code an approach based on the level of knowledge where various information on history, geometry, materials and monitoring of existing constructions are integrated and correlated with safety coefficients [4].

In this scenario, the assessment of onsite testing plays a relevant role in the identification of the construction; however, the local characteristics of several tests (i.e. double flat-jack test) do not provide complete information for a satisfactory evaluation of the structural behavior. Structural health monitoring, in particular ambient vibration test (AVT), provide a global characterization of the dynamic characteristics by considering the response of the entire construction to random external forces.

This paper, through the case study of San Filippo Neri's church, aims to propose an integrated approach in order to update and tune up numerical models of historical masonry buildings.

## 2 SAN FILIPPO NERI IN MACERATA

### 2.1 The construction of the building

Macerata is located in central Italy at 315 meters above sea level; the historical center is positioned on the top of a hill and it has maintained over the years its original structure such as the boundary wall defined in the Renaissance period and the widespread historical masonry buildings erected between the 16<sup>th</sup> and 19<sup>th</sup> centuries. The Church of San Filippo was commissioned by Cardinal Taverna in 1606 to complete the urban intervention which connected Piazza della Libertà to Piazza Vittorio Veneto [5]. The building is positioned on a slight slope between Corso della Repubblica and Via Santa Maria della Porta as it is showed in Figure 1.

In 1689, the Filippini's congregation asked to architect Giambattista Contini, a project for the construction of a new church. In the same year, Contini proposed his project but his design was criticized as too expensive and innovative. On the 28<sup>th</sup> of November 1697, another project by architect Ludovico Gregoriani was accepted and the first stone was laid in the month of December. During the construction operations the two contracting supervisors (Father Catenacci and Father Canelli) came into conflict with the Gregoriani, therefore Contini was recalled for the execution of a definitive project that included the Church and the annex convent. The work was completed in 1732 under the guidance of Sebastiano Cipriani, a pupil and collaborator of Contini [6].



Figure 1 San Filippo Neri in Macerata nowadays during the execution of the AVT

## 2.2 Historical evolution of the church

The church is formed by a rectangular narthex followed by the main oval aula, four radial chapels surround the aula which is surmounted by the elliptical dome with lantern.

In 1697, during the construction of the building, the original foundations were enlarged due to the consistency of the soil [7].

On the 29<sup>th</sup> of January 1899, an inspection was carried out in the basement of the adjacent house where it was discovered a cave with presence of inconsistent friable sandstone that extended under the church [8].

In 1903, engineer Canaletti ascertained the connection between the crack on the dome and the lowering of one of the piers. Canaletti's project considered the insertion of six iron stirrups on the large window over the entrance; furthermore, he exhorted the construction of a masonry vault inside the cave and its bricked up [9].

In 1929, two deep cracks protracted in the longitudinal direction; engineer Bonci's intervention consisted in an iron reinforcement ring under the drum to compensate the thrust of the dome [10].

In July 2012, the last restoration work included the strengthening of the dome with composite materials, the repair of vertical and sub-vertical cracks with traditional procedures and the installation of a steel reinforcement ring in the intrados of the drum (in Figure 2, highlighted in light blue the external tie beam connected to the encircling ring and the reinforcement tie on the lantern).

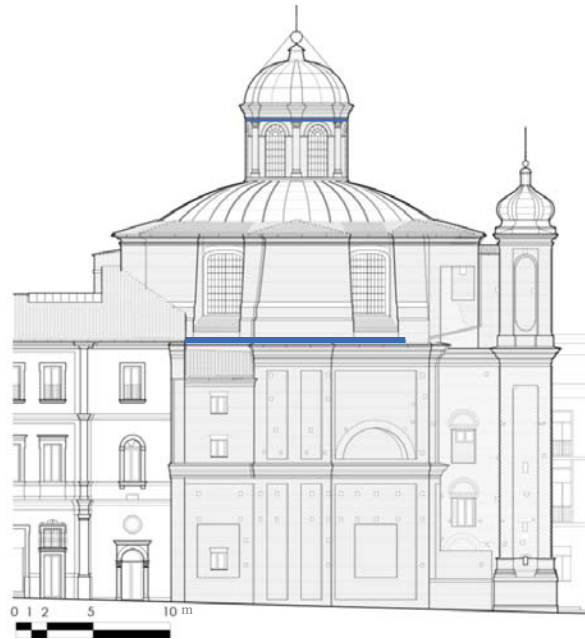


Figure 2 Northern lateral view of the church, in light blue the recent reinforcement interventions

### 2.3 Seismic history of the site

Since the 18<sup>th</sup> century, Macerata has been interested by several important seismic events (Figure 3).

On April 24, 1741; an earthquake of the VII grade involved the territory between Serrasanquirico and Fabriano, it had an extremely extensive damage area: from Pesaro and Urbino to Gubbio and Perugia, from Macerata to Fermo [11].

On the 1<sup>st</sup> of September 1951 an earthquake of 5,25 Moment Magnitude with epicenter in the Monti Sibillini struck the city of Macerata [12].

On September 4, 1997; a series of seismic events occurred in the area between Marche and Umbria. Three major shocks were recorded at 2:33 (Local Magnitude ML 5,5 and VII Mercalli-Cancani-Siebert MCS), at 11:40 (ML 5,8 and VIII-IX MCS) and at 11:46 (ML 4,7 and VII MCS), the serious and diffuse damaged area was identify with the Provinces of Perugia and Macerata [14].

On the 30<sup>th</sup> of October 2016 at 7:40, an earthquake of ML 6,5 interested the City of Macerata [15]; as reported by the technical office of the Diocese of Macerata-Tolentino-Recanati-Cingoli-Treia, in this occasion it was observed consistent damage to the dome of San Filippo Neri which caused the condemned of the building.

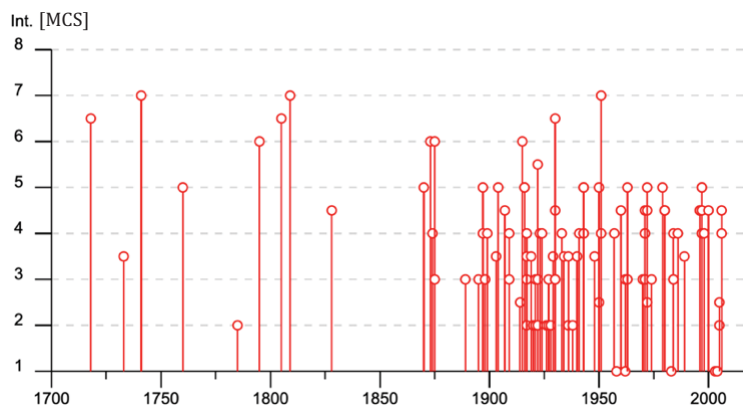


Figure 3 Seismic events in the period of interest [12]

### 3 ONSITE TESTING

In April and July 2018, the Laboratory of Proof and Research on Structures and Materials (PRiSMa) of the Architecture Department of University of Roma Tre carried on an extensive experimental campaign on the church of San Filippo Neri in order to investigate the structural elements, characterize the mechanical property of the masonry and identify the dynamic behavior of the construction.

During the onsite experimental campaign different tests were performed including:

- n° 20 video endoscopy inspections of the masonry elements
- n° 1 sonic tomography of the south-eastern pillar
- n° 3 double flat jack tests of the masonry
- n° 3 dynamic penetrometer tests of the mortar joints
- ambient vibration test

In the present paper are reported only the most relevant for the purpose of this research.

#### 3.1 Double flat jack test

Three double flat-jack tests were executed at the ground floor level of the building in order to estimate the elastic moduli of the brick masonry elements (Figure 4).

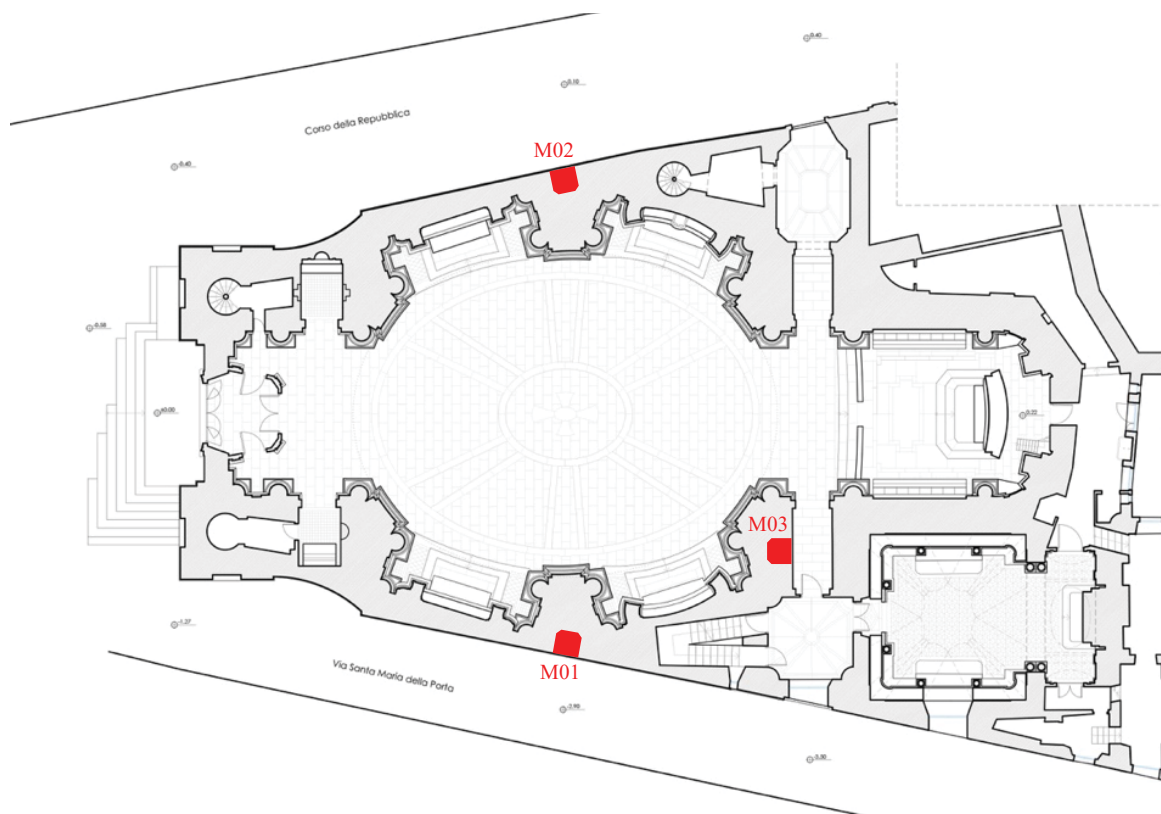


Figure 4 Double flat-jack test location

The double flat-jack test is a well-known slightly destructive technique; during the test two parallel slots are sawn into the mortar joints, then two flat-jacks are inserted into the slots finally the pressure is increased cyclically through a hydraulic pump. The elastic modulus of masonry is evaluated by measuring deformation due to the compressive stress.

The performed test is summarized in the following steps:

- 1) Set of the line cuts and holes to support the instrumentation;
- 2) Execution of the cuts with Husqvarna K960 Ring Saw;
- 3) Inserting of two flat-jack into the slots (dimensions 350 x 175 mm for the semi-circular shape plus 350 x 85 mm for the rectangular shape by 4 mm of thickness) and connection to pressure switch and 700 bar hydraulic pump;
- 4) Set of 3 displacement sensors Penny & Giles SLS130 in vertical direction and 1 in horizontal direction;
- 5) Connection of the equipment to data acquisition system National Instruments SCXI 1001 with SCXI 1314/1520 slot and NI SCXI-1600 analog to digital converter with 16-bit resolution;

The tests were executed in different loading cycles, the stress state was evaluated with (1) according to [16].

$$\sigma = P \cdot K_m \cdot K_a \tag{2}$$

$P$  is the flat-jack pressure in MPa;

$K_m$  is a constant dependent on geometry and stiffness of the flat-jack;

$K_a$  is a constant dependent on the ratio between the areas of the flat-jack and the slot;

The results of the tests are reported in Table 1.

Test	Elastic Modulus [MPa]	Poisson's coefficient [-]
M01	4160,7	0,21
M02	7440,6	0,30
M03	2896,1	0,20

Table 1 Double flat-jack test results

### 3.2 Ambient vibration test

Ambient vibration measurements and output-only dynamic testing are consolidated techniques for dynamic characterization of historical masonry constructions [17]. The test was conducted on the church in July 2018, the response acceleration of the construction was recorded for about 1 hour by 16 accelerometers located in 7 points at two different heights (Figure 5, Figure 6).

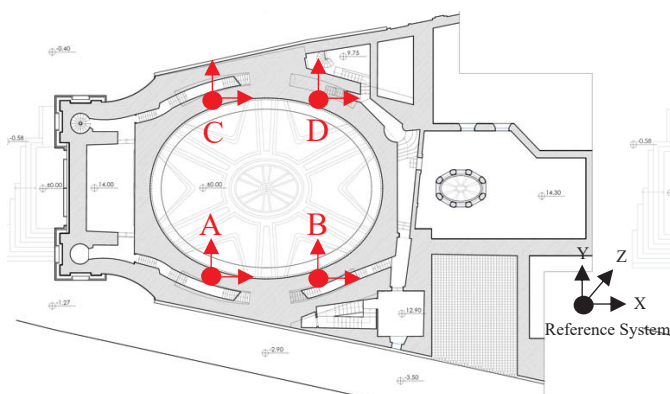


Figure 5 AVT accelerometers setting at 15 m

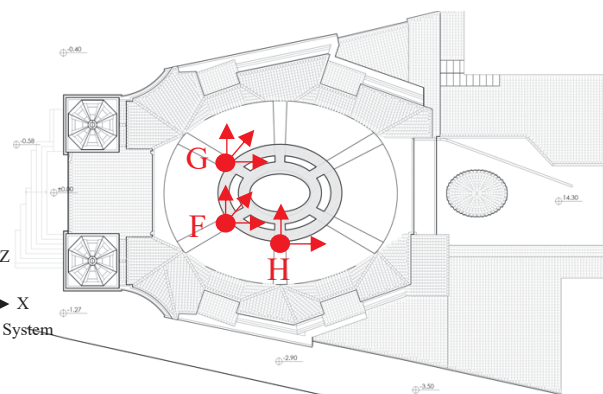


Figure 6 AVT accelerometers setting at 25 m

The sensors were connected to two different 24-bit acquisition systems, each one equipped with 2 signal conditioners, 8 channels and 8 independent A/D converters. The two systems are provided with GPS antenna to record the data on absolute time and synchronize the acquisitions. The measures were recorded with 200 Hz sample frequency with dedicated anti-aliasing filter using 16 uniaxial ICP piezoelectric accelerometers (n° 9 PCB 393A03, 1 V/g sensitivity, range  $\pm 5$  g, 10  $\mu\text{g}$  rms resolution and n° 7 PCB 393B12, 10 V/g sensitivity, range  $\pm 0,5$  g, 8  $\mu\text{g}$  rms resolution).

## 4 OPERATIONAL MODAL ANALYSIS

Operational modal analysis is based on the assumption of white noise random vibrations; in this scenario, it is sufficient to analyze the response of the structure to unknown random vibration (output-only modal identification) to extract the modal parameters of the building (natural frequencies, modal shape vectors and modal damping).

The extraction of modal parameters from ambient vibration data was carried out by using the polyreference least-squares complex frequency-domain method [18], explained in 4.1.

### 4.1 PolyMAX method

The method is based on the processing of the Cross-power spectrum functions- $S_{xy}(j\omega)$  which are correlated with the frequency response function-FRF of the system and expressed as function of modal parameters.

The data recorded are represented in the z-domain (2):

$$z = e^{j\omega\Delta t} \quad (2)$$

$\Delta t$  is the sampling time.

$\mathbf{H}(\omega)$  is the matrix containing the FRFs between all  $m$  inputs and  $l$  outputs (3).

$$[\mathbf{H}(\omega)] = \sum_{\gamma=0}^p z^\gamma [\beta_\gamma] \cdot \left( \sum_{\gamma=0}^p z^\gamma [\alpha_\gamma] \right)^{-1} \quad (3)$$

$\mathbf{H}(\omega)$ ,  $[\beta_\gamma]$ ,  $[\alpha_\gamma] \in \mathbb{C}^{l \times m}$ ;  $[\beta_\gamma]$  are the numerator matrix polynomial coefficients;  $[\alpha_\gamma]$  are the denominator matrix polynomial coefficients;  $p$  is the model order.

Once the denominator coefficients  $[\alpha_\gamma]$  are determined, the poles and modal participation factors are retrieved as the eigenvalues and eigenvectors of their companion matrix.

Pole-residue model is considered in (4).

$$[\mathbf{H}(\omega)] = \sum_{i=0}^n \frac{\{v_i\} \langle l_i^T \rangle}{j\omega - \lambda_i} + \frac{\{v_i^*\} \langle l_i^H \rangle}{j\omega - \lambda_i^*} - \frac{[LR]}{\omega^2} + [UR] \quad (4)$$

$n$  is the number of modes;  $\{v_i\} \in \mathbb{C}^l$  are the mode shapes;  $*$ ,  $T$ ,  $H$  respectively denote complex conjugate, transpose and complex conjugate transpose of a matrix.

$\langle l_i^T \rangle \in \mathbb{C}^m$  are the modal participation factors and the poles, which are occurring in complex-conjugated pairs, are related to eigenfrequencies  $\omega_i$  and damping ratios  $\xi_i$ .

$$\lambda_i, \lambda_i^* = -\xi_i \omega_i \pm j \sqrt{1 - \xi_i^2} \omega_i \quad (5)$$

$[LR]$ ,  $[UR] \in \mathcal{M}^{l \times m}$  are respectively the lower and upper residuals which model the influence of the out-of-band modes in the considered frequency band. The interpretation of the

stabilization diagram yields a set of poles  $\lambda_i$  and corresponding participation factors  $\langle l_i^T \rangle$ . Since the mode shapes  $\{v_i\}$  and the lower/upper residuals are the only unknowns, they are readily obtained by solving the equation in a linear least-square sense [20].

The PolyMAX method is implemented in the software Simcenter TestLab 18 [20] which was used in this work for the data processing.

#### 4.2 Data processing and results

For the visualization of the results, it was considered a geometric model, defined in Figure 7.

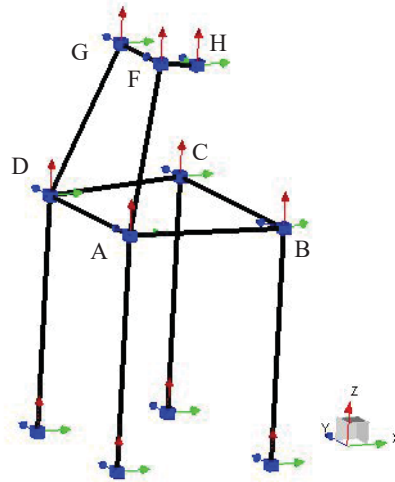


Figure 7 Geometric model

In the pre-processing stage, there was applied a high-pass filters to the recorded accelerations in order to reduce the noise of the electronic devices. Thereafter, the Cross-power spectra were elaborated with 0,049 Hz frequency resolution and 5% windowing; for the identification of the global modes there were considered as reference the measurements recorded in node B and C while for the identification of the local modes of the dome the measurements recorded in node G.

The PolyMAX algorithm was run on different sets of Cross-power spectra to investigate the stable poles and estimate the modal characteristics of the construction.

In Table 2 are reported the experimental results of the operational modal analysis.

Mode 1	2,065 Hz	$\xi=1,11\%$	Mode 2	2,972 Hz	$\xi=2,84\%$	Mode 3	3,395 Hz	$\xi=1,45\%$

Mode 4	4,176 Hz	$\xi=1,27\%$	Mode 5	5,185 Hz	$\xi=1,53\%$	Mode 6	5,342 Hz	$\xi=1,14\%$
Mode 7	6,878 Hz	$\xi=3,14\%$	Mode 8	7,773 Hz	$\xi=1,81\%$	Mode 9	11,228 Hz	$\xi=1,37\%$

Table 2 Experimental Modes

The results identify 1<sup>st</sup> and 2<sup>nd</sup> modes with the global translation respectively in Y and X direction, 3<sup>rd</sup> mode involves the global rotation of the church while 4<sup>th</sup> mode the rotation of the back of the church; 5<sup>th</sup> and 6<sup>th</sup> modes identify the global translational modes with in-plane deformation.

7<sup>th</sup>, 8<sup>th</sup> and 9<sup>th</sup> modes are local modes proper of the dome; 7<sup>th</sup> mode identify the translation of the dome in the Y direction, 8<sup>th</sup> mode has a prevalent deformation in the vertical direction while 9<sup>th</sup> mode identify the translation of the dome in the X direction.

## 5 GLOBAL FINITE ELEMENT MODEL

A numerical tridimensional model of the construction was built with the finite element software Midas Fea [21]. The model was based on accurate geometrical survey which allowed detailed representation of the volumes. There were considered 546049 3D-solid elements to model the masonry and 129 1D-elements for the steel reinforcements. The reinforced concrete floors of the annex building and the eastern roof of the church were modeled with relative constrains while the influence of the annexed building complex was taken into account with horizontal restrains. The model considers tridimensional translational restrains for the base nodes; lateral nodes on the ground-masonry interface were restrained only in the horizontal directions; in Figure 8 it is shown the FEM used for the analysis.

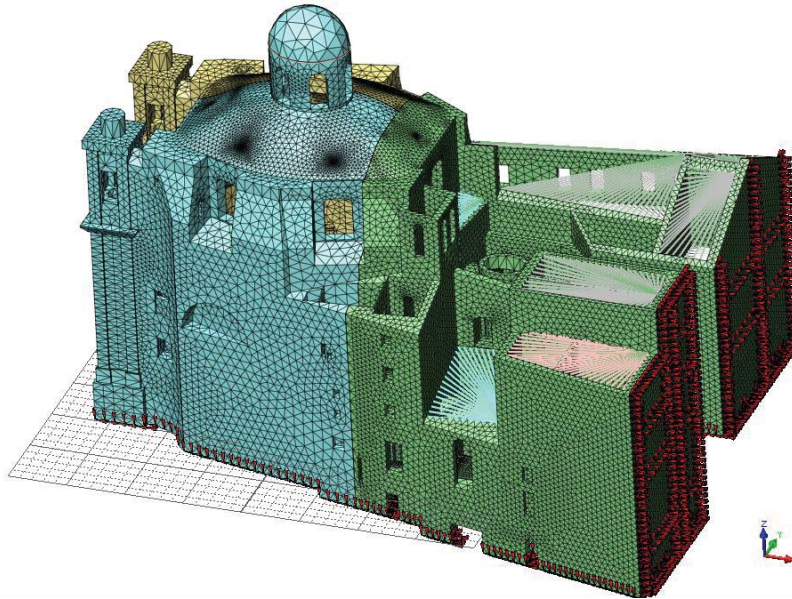


Figure 8 FEM model

The materials were considered homogeneous and isotropic with elastic behavior. The FEM was divided in three main macro zones in order to assign different characteristics to the materials; for the mass density there were assumed the values suggested by the Italian code [22] as reported in Table 3.

Material	Mass density [kN/m <sup>3</sup> ]	E [MPa]	$\nu$ [-]
Southern masonry – E1	18	4160,7	0,21
Northern masonry – E2	18	7440,6	0,30
Eastern masonry – E3	18	2896,1	0,20
Steel reinforcements	76,98	210000	0,3

Table 3 FEM materials

### 5.1 Model updating

On the basis of the experimental results, it was carried on sensitivity analysis in order to match numerical modal analysis with operational modal analysis. Considering the complexity of the building and the uncertainties related with the construction technology (especially in the dome), the analysis focused on the identified global modes of the church (first six modes of vibrations). The updating procedure of the model was based on the evaluation of two main quantities well known in the scientific literature [23]:

The relative frequency error ( $Df_{i,j}$ ), defined in (6).

$$Df_{i,j} = \frac{|f_{num,i} - f_{exp,j}|}{f_{exp,j}} \cdot 100 \quad (6)$$

$f_{num,i}$  is the numerical frequency and  $f_{exp,i}$  the experimental frequency for the  $i^{\text{th}}$  mode of vibration.

The modal assurance criterion (MAC) [24], defined in (7).

$$MAC \left( \left\{ \phi_{num,i} \right\}, \left\{ \phi_{exp,j} \right\} \right) = \frac{\left| \left\{ \phi_{num,i} \right\}^T \left\{ \phi_{exp,j} \right\} \right|^2}{\left( \left\{ \phi_{num,i} \right\}^T \left\{ \phi_{num,i} \right\} \right) \left( \left\{ \phi_{exp,j} \right\}^T \left\{ \phi_{exp,j} \right\} \right)} \quad (7)$$

$\phi_{num,i}$  is the numerical modal vector and  $\phi_{exp,i}$  is the experimental modal vector for the  $i^{\text{th}}$  mode of vibration.

On the basis of  $D_f$  and MAC between each numerical and experimental mode, it was implemented a procedure in order to select the proper numerical mode.

The process is summarized in the following steps:

1. Identification of the numerical frequency ( $f_{num,i}$ ) closest to experimental frequency ( $f_{exp,i}$ );
2. Selection of the interested range of numerical modes [ $f_{num,i-4}$ ,  $f_{num,i+4}$ ];
3. Normalization of the relative frequency error with the maximum error in the interested range defined in (8);

$$Dnf_{i,j} = \frac{Df_{i,j}}{\max[f_{num,i-4}, f_{num,i+4}]} \quad (8)$$

4. Selection of the suitable  $i^{\text{th}}$  numerical mode on the base of the minimum error defined in (9);

$$error_{i,j} = 0,5 Dnf_{i,j} + (1 - MAC_{i,j}) \quad (9)$$

Model updating started with the identification of the proper boundary conditions.

The updated models considered 3-D point spring elements according to Winkler's theory of elastic foundations. The spring stiffness was modified within a range of reasonable values on the base of the moduli of subgrade reaction (ks) available in literature [25].

Three different sets of springs were considered in the global finite element model:

- 10 XY – Z (ks in horizontal direction 10 times than vertical direction)
- XYZ (equal ks in the three directions)
- 0,1 XY – Z (ks in horizontal direction 10% than vertical direction)

Sensitivity analysis of the three sets was carried on within a range of ks between 14400 and 36000 kN/m<sup>3</sup>; the results are reported in Figure 9, Figure 10 and Table 4.

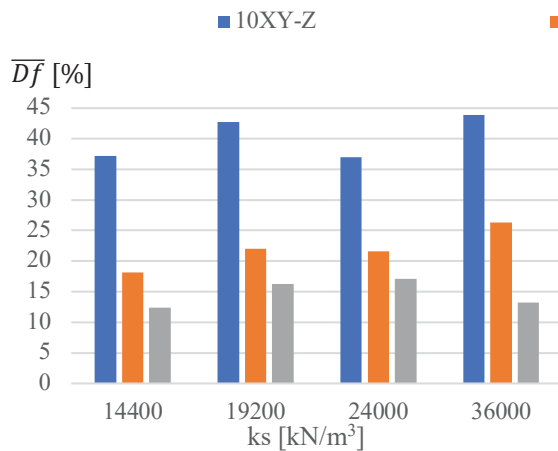


Figure 9 Average relative frequency error

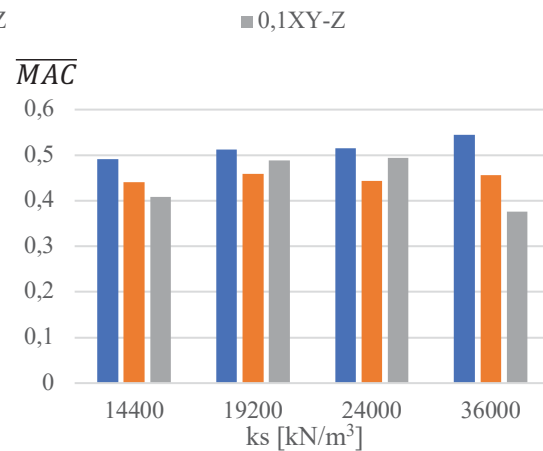


Figure 10 Average MAC

The average errors for the three sets of models were calculated according to (9);

$k_s$ [kN/m <sup>3</sup> ]	10XY-Z	XYZ	0,1XY-Z
14400	1,19	0,89	0,82
19200	1,14	0,88	<b>0,76</b>
24000	1,14	0,94	0,81
36000	1,15	0,96	0,83

Table 4 Average error for the three sets of models

Model 0,1 XY – Z with  $k_s$  equal to 19200 kN/m<sup>3</sup> corresponds to the minimum error thus it was selected as first updating step.

Material characterization was further investigated by carrying sensitivity analysis on the moduli of elasticity of the masonry; the reference values of the moduli were modified within reasonable range, the parameters were varied one at the time in order to highlight their influence on the modal behavior of the building.

The following graphs report frequency error and MAC of the first six modes of vibrations on the variation of modulus of elasticity.

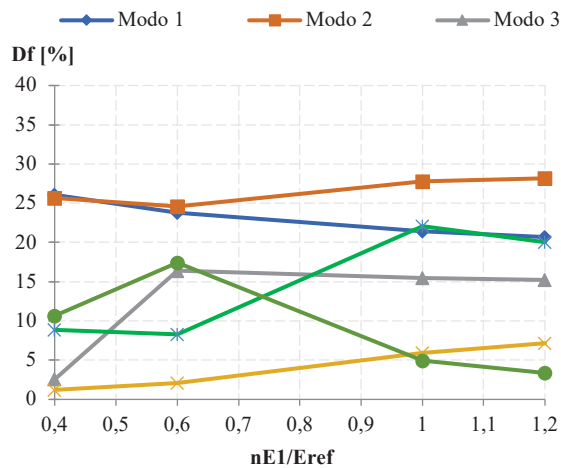


Figure 11 Frequency error vs E1 variation

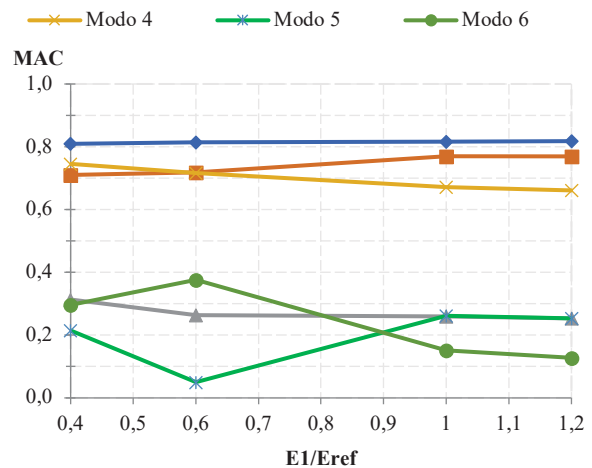


Figure 12 MAC vs E1 variation

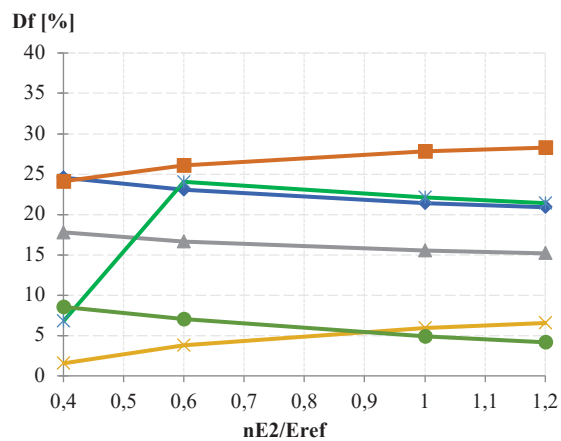


Figure 13 Frequency error vs E2 variation

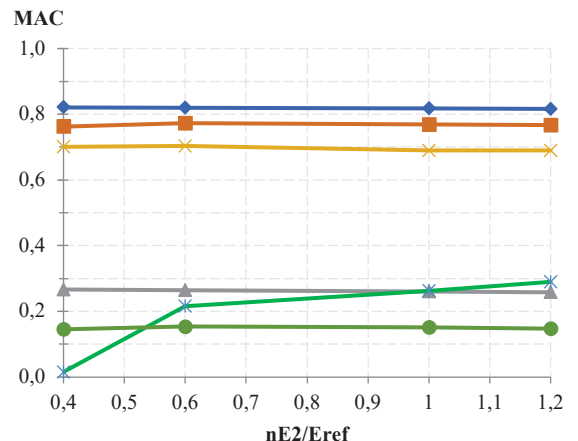


Figure 14 MAC vs E2 variation

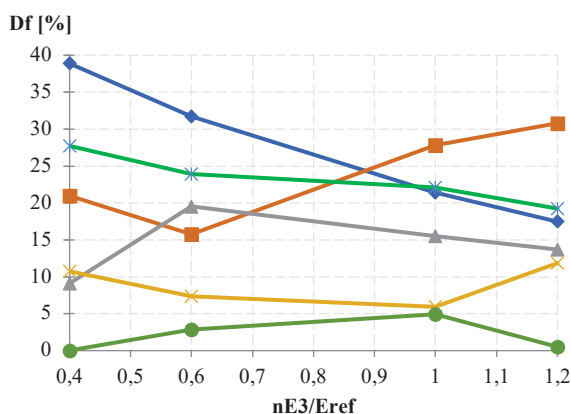


Figure 15 Frequency error vs E3 variation

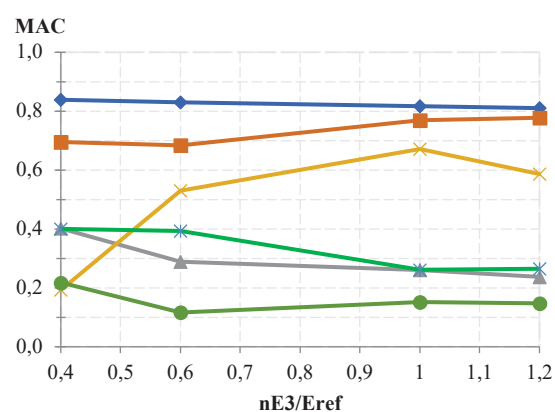


Figure 16 MAC vs E3 variation

Sensitivity analysis highlighted the influence of modulus of elasticity on certain modes.

Variation of the elasticity of the southern masonry (E1) showed the main influence on the modal deformations of 5<sup>th</sup> and 6<sup>th</sup> mode (Figure 12) while frequency errors of 3<sup>rd</sup>, 4<sup>th</sup> and 5<sup>th</sup> mode decrease with the reduction of elasticity (**Errore. L'origine riferimento non è stata trovata.**). Northern masonry (E2) stiffness variation conditioned mainly the behavior of 5<sup>th</sup> mode of vibration (Figure 13 and Figure 14).

Variation of the eastern masonry (E3) elasticity affected mainly modal deformation of 4<sup>th</sup> mode (Figure 16) and frequency error of the first two modes of vibration (Figure 15).

According to the previous considerations, the model updating suggests:

- strong reduction of elasticity in the southern masonry (E1) in order to decrease the frequency error;
- slight increasing of the northern masonry elasticity (E2) in order to raise MAC of the 5<sup>th</sup> mode
- small reduction of the eastern masonry elasticity (E3) to increase 5<sup>th</sup> mode MAC and decrease 2<sup>nd</sup> and 6<sup>th</sup> mode frequency error.

## 5.2 Discussion

According to the influence of elasticity on the modal parameters, three different tuned up models are proposed in agreement with the updating procedure.

- model 0 is the initial fixed base model
- model 1 is the elastic foundation model with masonry elasticity from double flat-jack results
- model 2 is the updated model with minimum average frequency error
- model 3 is the updated model with maximum average MAC

In Table 5 are reported the set of parameters of each model.

Model	Foundation [N/mm]		Modulus of elasticity [N/mm <sup>2</sup> ]			Mass density [kN/m <sup>3</sup> ]
	ks,xy	ks,z	E1	E2	E3	Masonry
0	-	-	4160,7	7440,6	2896,1	18
1	333,7	3336,7	4160,7	7440,6	2896,1	18
2	333,7	3336,7	1664,3	7440,6	2896,1	18
3	333,7	3336,7	2704,4	8184,7	2606,5	18

Table 5 Model parameters

The updating procedure highlighted the necessity to reduce the stiffness of the southern masonry; this result is in accordance with the historical events which reported the settlement problems of the building. The result from the double flat jack offered reliable information on the materials, moreover the introduction of elastic foundation provided a better match between experimental and numerical behavior.

The model updating underlined the enhancing of the error quantities with the variation in the relationship between the modulus of elasticity in particular for the higher modes (4<sup>th</sup>, 7<sup>th</sup> and 8<sup>th</sup> mode).

The final results from each model are presented in Table 6 and Table 7.

Df [%] Model	Modes of vibration									$\overline{Df}$	
	1	2	3	4	5	6	7	8	9	1to9	1to6
0	110,82	115,93	125,24	88,04	82,93	101,50	71,23	14,89	8,76	79,93	104,08
1	21,40	27,79	15,51	5,93	22,07	4,93	1,24	16,62	0,89	12,93	16,27
2	24,55	24,11	17,78	1,55	6,78	8,54	0,05	1,95	0,44	<b>9,53</b>	<b>13,89</b>
3	25,16	23,69	16,94	0,18	13,24	17,43	2,01	4,08	10,49	12,58	16,11

Table 6 Relative frequency error of the models

MAC Model	Modes of vibration									$\overline{MAC}$	
	1	2	3	4	5	6	7	8	9	1to9	1to6
0	0,89	0,73	0,11	0,13	0,69	0,47	0,55	0,44	0,31	0,48	0,51
1	0,82	0,77	0,26	0,67	0,26	0,15	0,22	0,60	0,22	0,44	0,49
2	0,82	0,76	0,27	0,70	0,02	0,15	0,47	0,72	0,18	0,45	0,45
3	0,82	0,74	0,28	0,76	0,11	0,40	0,41	0,59	0,55	<b>0,52</b>	<b>0,53</b>

Table 7 Model Assurance Criterion of the models

## 6 CONCLUSIONS AND FUTURE WORK

The results from the experimental campaign on the church of San Filippo Neri in Macerata were reported and discussed. The flat-jack test reported a significant diversity in the modulus of elasticity of the masonry: northern masonry was identified with the stiffer material followed by the southern masonry and then eastern masonry. The results from the static tests provided reliable information on the materials, moreover the relationship between elastic moduli was partially validated by the numerical modal analysis of the FEM.

Ambient vibration test and operational modal analysis were confirmed as appropriate techniques for the evaluation of the dynamic response of historical masonry construction; furthermore, the PolyMAX method allowed an accurate identification of the global dynamic behavior of the construction as well as the local behavior of large structural elements such as the dome. The updating procedure highlighted the complexity of the problem in the optimum selection of the parameters; the application of elastic foundations was confirmed to be the most relevant upgrade in order to match numerical and experimental modal behavior.

Model upgrading suggested the additional reduction of stiffness in the southern area of the church, the goal was pursued by decreasing the elasticity of the southern masonry; however, a more sophisticated path (such as the local variation of the spring elasticity) could have been followed in order to match the experimental dynamic behavior although the complexity of the problem returns the attempt to a future development. The upgrading procedure and the introduction of a criteria in the selection of numerical modes set the groundwork for a future automated model upgrading able to handle higher number of parameters.

## ACKNOWLEDGEMENTS

The authors are grateful to Eng. Giorgio Sforza and Eng. Lorenzo Lepori from Essebi srl for the support during the ambient vibration test and the operational modal analysis.

Arch. Enrico Da Gai and Eng. Francesco Pipoli from Studio Da Gai Architetti are acknowledged for the assistance in the geometrical survey.

The authors thank Arch. Lorena Sguerri and Giovanni Barco from the PRiSMa laboratory for the cooperation and availability during the testing campaigns.

## REFERENCES

- [1] C. B. L. D. C. N. S. S. Fiorentino Gabriele, «Damage patterns in the town of Amatrice after August 24th 2016 Central Italy earthquakes,» *BULLETIN OF EARTHQUAKE ENGINEERING*, pp. 1399-1423, 2018.
- [2] C. Baggio, «Il restauro antisismico dei centri storici e la regola d'arte,» *Ricerche di Storia dell'Arte*, 2010.
- [3] M. C. G. G. L. P. Pere Roca, «Structural Analysis of Masonry Historical CONstructions. Classical and Advanced Approaches,» *Arch Computer Methods Eng*, vol. 17, p. 299, 2010.
- [4] S. S. V. I. Nuti Camillo, «Seismic assessment of the molise hospital and upgrading strategies,» in *13th World Conference on Earthquake Engineering*, Vancouver, B.C., Canada, 2004.
- [5] Ministero per i Beni e le Attività Culturali, *Linee Guida per la valutazione e riduzione del rischio sismico del patrimonio culturale*, Gangemi Editore, 2010.
- [6] Archivio Priorale di Macerata, *Instrumentorum*, n. 858, Macerata: Archivio di Stato di Macerata (ASM), 1606-1609.
- [7] A. D. Bufalo, G. B. Contini e la tradizione del tardomanierismo nell'architettura tra '600 e '700, Roma: Edizioni Kappa, 1982.
- [8] E. Bettucci, *La prima chiesa dedicata in tutto il mondo a S. Filippo Neri dopo la sua canonizzazione*, Macerata, 1894.
- [9] A. Canaletti, «Perizia geotecnica del 9 febbraio 1899,» Archivio della Confraternita delle Stimmate di San Francesco, Macerata, 1899.
- [10] A. Canaletti, «Relazione sulla causa delle lesioni nella cupola della Chiesa di San Filippo e computo metrico dei restauri spettanti alla Ven. Confraternita delle Stimmate,» Archivio della Confraternita delle Stimmate di San Francesco, Macerata, 1903.
- [11] G. Bonci, «Progetto di restauro parziale interno della Chiesa di S. Filippo Neri in Macerata - Relazione finale sull'opera,» Archivio della Confraternita delle Stimmate di San Francesco, Macerata, 1929.
- [12] Monachesi, «Principali terremoti storici dell'area umbro-marchigiana,» Istituto Nazionale di Geofisica e Vulcanologia, 1987. [Online]. Available: <https://emidius.mi.ingv.it/GNDT/T19970926/schede1279-1879.html>.
- [13] C. C. Andrea Tertulliani, «Il terremoto del 1 settembre 1951 nel maceratese: nuove fonti e revisione macrosismica,» *Quaderni di Geofisica*, n. 147, p. 11, 2018.
- [14] R. Camassi, «Macroseismic survey of the 1997-1998 Umbria-Marche earthquakes: from practice to practice,» Barba et al., Rome, Italy, 2007.

- [15] Gruppo di Lavoro INGV sul Terremoto in centro Italia, «Rapporto di sintesi sul Terremoto in centro Italia Mw 6.5 del 30 ottobre 2016,» 2016.
- [16] L. M. C. R. L. B. G. P. Rovida A., «CPTI15, the 2015 version of the Parametric Catalogue of Italian Earthquakes,» Istituto Nazionale di Geofisica e Vulcanologia, 2016. [Online]. Available: <http://doi.org/10.6092/INGV.IT-CPTI15>.
- [17] American Society fo Testing and Materials, «Standard test method for in situ measurement of masonry deformability properties the using flat-jack method, C 1197-09,» ASTM, Philadelphia, 1991.
- [18] E. M. P. C. Alessandro De Stefano, «Structural health monitoring of historical heritage in Italy: some relevant experiences,» *J Civil Struct Health Monit*, n. 106, p. 88, 2016.
- [19] H. V. d. A. P. G. a. J. L. Bart Peeters, «The PolyMAX frequency-domain method: a new standard for modal parameter estimation?,» *Shock and Vibration*, vol. 11, 2004.
- [20] LMS International, The LMS Test.Lab Modal Analysis manual, 2012.
- [21] S. I. S. NV, «Simcenter Testlab Version 18.0,» 2018.
- [22] M. I. T. Co., «Midas FEA 2016 (v1.1),» 2015.
- [23] Ministero delle Infrastrutture e dei Trasporti, «Circolare n. 617 C.S.LL.PP.,» Gazzetta Ufficiale della Repubblica Italiana, Roma, 2009.
- [24] B. D. Allemang RJ, «A correlation coefficient for modal vector analysis,» in *Ist international modal analysis conference*, Orlando, 1982.
- [25] B. J. E., *Foundation analysis and design*, USA: McGraw-Hill, 1996, pp. 121-127, 501-509.